Hereby I report the most important results of the NKFI K116228 project following the same order as it was given in the original Workplan.

I. Characterization of the structural and functional consequences of the novel and other potentially interesting mutations at molecular level

Our aim was to give a better insight into the genotype-phenotype and structural-functional relationships in the deficiencies of the natural anticoagulants. We have built up databases for AT, protein C (PC) and protein S (PS) deficiencies. Besides laboratory parameters of AT, PC and PS levels and results of mutation analysis clinical parameters including the presence or absence of thrombotic event(s), age at the first clinical event, age at diagnosis of AT/PC/PS deficiency, presence or absence of other inherited thrombotic risk factors and provoking factors and the therapeutic modality have been collected and introduced into these databases. At present, according to our knowledge, our study group has one of the largest clinical-laboratory-genetic database of AT, PC and PS deficiency by which we could join to international databases coordinated by the International Society of Thrombosis and Haemostasis (ISTH). At present data of n=446 AT deficient patients, n=173 PC deficients and n=72 PS deficient patients, all confirmed by genetic studies are available. (During the study period more than 1500 individuals with suspected AT/PC/PS deficiency were screened.)

We have focused especially on antithrombin (AT) deficiency due to the relatively large number of AT deficient patients in Hungary. We aimed to investigate the genetic background of this relatively high frequency, to draw conclusions on the impact of different types and subtypes of AT deficiency on clinical and laboratory phenotype by recruiting one of the largest AT deficient patient population worldwide. We aimed to explain the molecular mechanism by which AT Budapest 3 (ATBp3), the most common mutation in Hungary, leads to AT deficiency. A reliable laboratory protocol for AT deficiency diagnosis was introduced. Novel, or previously uncharacterized mutations were investigated by in vitro protein expression and biochemical methods and by in silico analysis. In details:

1, Clinical and laboratory aspects of AT deficiency based on population studies and case reports.

Until recently, a total of 329 non-related AT deficient patients (index patients) and their family members (total n=446) were recruited by our study group. AT activity was determined by chromogenic assay based on factor Xa-inhibition in the presence of heparin and also in the absence of heparin (progressive AT activity, developed by us in the previous research period, OTKA_PD101120) on Siemens BCS-XP coagulometer. The AT antigen (AT:Ag) concentration was measured by immunonephelometry (Siemens, N Antiserum to Human Antithrombin III). All patients were genotyped for *SERPINC1* mutation. Sanger sequencing was executed to identify mutations in the exons, the flanking intronic regions and in the promoter of *SERPINC1* gene using an ABI3130 Genetic Analyzer and Sequencing Analysis 5.4 software (Thermo Fisher Scientific, Carlsbad, CA, USA). If Sanger sequencing did not find causative mutations, multiplex ligation-dependent probe amplification (MLPA) was performed using SALSA MLPA KIT P227 (MRC-Holland, Amsterdam, the Netherlands) using an ABI3130 Genetic Analyzer. The MLPA products were analyzed by GeneMapper Software 4.1. By the time of this report we have identified 39 different *SERPINC1* mutations with high mutation

detection rate (98%). Among the 39 mutations 18 novel ones were detected (Figure 1). Most of the index patients carried type II heparin-binding-site (HBS) mutations (85% of all types) due to the high frequency of ATBp3 (85% out of type IIHBS). ATBp3 was registered in homozygous and heterozygous forms, while all other *SERPINC1* mutations were detected only in heterozygous state.

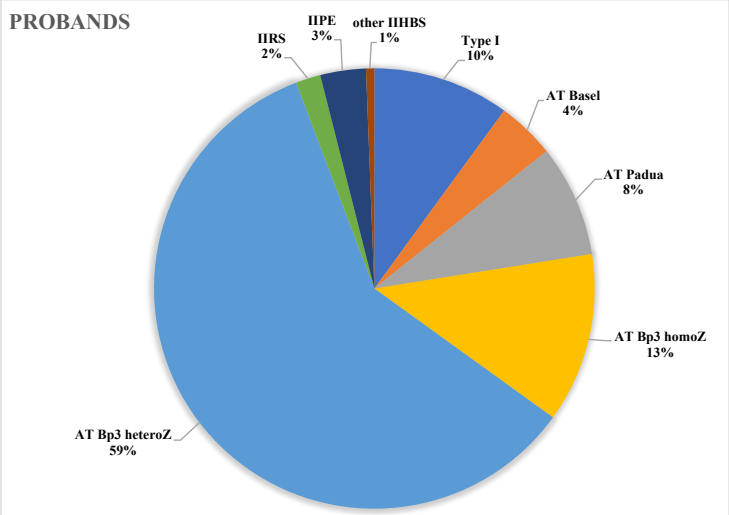

Figure 1. Distribution of *SERPINC1* mutations among AT deficient patients.
Type II HBS mutations: AT Bp3, AT Budapest 3, p.Leu131Phe; AT Basel, p.Pro73Leu; AT Padua, p.Arg79His. IIRS, type II reactive site mutations; IIPE, type II pleiotropic effect mutations. Percentage values represent the frequency of patients within a mutation group.

Clinical data including arterial and venous thrombotic symptoms (ATE and VTE), pregnancy-related complications and demographic data were registered. Presence of thrombosis provoking factors was considered if trauma, surgery, hospitalization due to acute illness, central venous catheters, immobilization, pregnancy, oral anticoncipient, hormonal treatment, prolonged travel, L-Asparaginase treatment occurred within one month before the diagnosis of VTE. The presence of acquired risk factors (i.e. chronic situations as malignancy, paroxysmal nocturnal hemoglobinuria, autoimmune diseases, antiphospholipid syndrome, obesity, as BMI above 30kg/m^2, varicose veins, nephrotic syndrome, heart failure, long-term immobilization) was also registered. Concerning the clinical consequences of AT mutations type I deficiency in general was associated with a severe venous thrombotic phenotype in our cohort, except for AT Wobble, in which case no VTE but MI was registered. Type IIHBS is an interesting group of AT deficiency, where the clinical and laboratory phenotypes are more heterogeneous and dependent on the specific mutation. ATBp3, AT Padua I and AT Basel associated with not only VTE but also ATE and pregnancy complications were also registered with different frequencies (*Gindele et al. Thromb Res 2017;160:119-128*). When the time to the first manifestation of VTE was considered as a measure of clinical severity, it is to be highlighted that type I AT deficiency was more severe than heterozygous IIHBS deficiency, however ATBp3 homozygosity was more severe than type I AT deficiency in this aspect. Within type IIHBS group ATBp3 homozygosity was the most severe and ATBp3 heterozygosity was significantly more severe than AT Padua I. AT Basel and AT Padua I were not significantly different concerning the time to the first manifestation of VTE. When the time to first manifestation of a composite clinical endpoint including not

only VTE but also ATE and pregnancy complications was taken into consideration, the severity of type I and type IIHBS heterozygotes did not differ significantly. ATBp3 homozygosity was more severe than type I and type IIHBS heterozygous AT deficiency in this aspect. AT Basel was rather associated with arterial thrombotic events (ATE); the highest number of pregnancy complications was detected in AT Padua I (Figure 2).

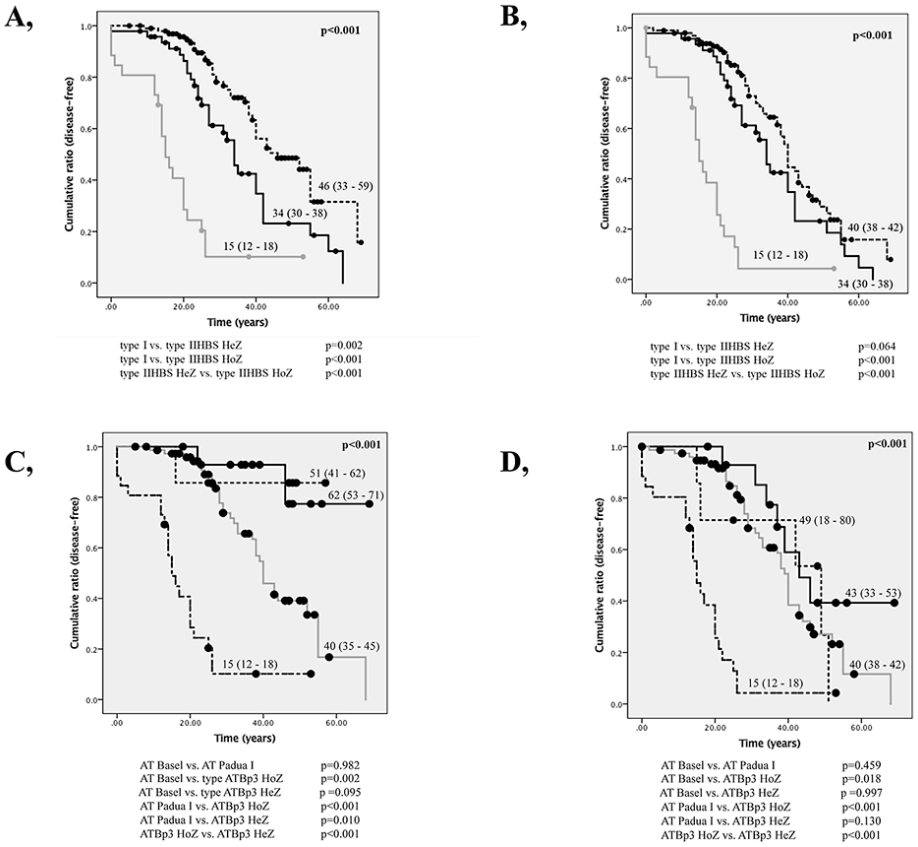

Figure 2. Comparison of time to the first manifestation of venous thrombosis (A and C) and to the first manifestation of any thrombotic event (B and D) in type I, type IIHBS heterozygotes and in ATBp3 homozygotes.

Kaplan-Meier survival curves illustrate the difference among type I (black solid line, n=47), type IIHBS heterozygotes (dotted line, n=98) and ATBp3 homozygotes (grey solid line, n=26) for venous thrombosis (A) and for any thrombotic event (B) including venous and arterial thrombosis and pregnancy complications. The differences in time to the first clinical event among the different type IIHBS groups for venous thrombosis (C) and for any thrombotic event (D) are also demonstrated. AT Basel (n=7) is represented with a dotted line, AT Padua I (n=15) is represented with a black solid line, ATBp3 heterozygotes (n=76) are represented with a grey solid line and ATBp3 homozygotes (n=26) are represented with a semi-dotted line. Cumulative ratio on the y-axis represents the ratio of individuals without clinical event. Censored cases are marked with circles. The median values of the time at the first clinical event (years) with the 95% Confidence Intervals in the brackets are shown in the figures.

HeZ, heterozygote; HoZ, homozygote

As most of the patients carried type IIHBS mutations in our study population, we investigated genotype and phenotype associations in this group in more details afterwards by recruiting more patients and by starting collaboration with the thrombosis goups of the University of Novi Sad and the University of Belgrade, Serbia. Genotype-phenotype

associations were demonstrated by case-reports and case-series. We reported pregnancy-related stroke in a female, early onset abdominal venous thrombosis in a newborn, both were homozygous for the ATBp3 mutation (*Kovac et al. Thromb Res 2016;139:111-113; Kovac et al. Blood Coag Fibrinol 2017;28:264-266*). We investigated the association of different AT mutations with pregnancy complications in a retrospective analysis of 28 females with 64 pregnancies and concluded that ATBp3 homozygosity conferred the most severe risk for adverse pregnancy outcome. The pregnancy-related VTE did not differ between type I and type II deficiencies, however in homozygous ATBp3 deficiency all untreated pregnancies had an unfavorable outcome with late pregnancy loss as the most common consequence (*Kovac et al. Thromb Res 2019;173:12-19*). Pediatric population represents another special patient group in which special considerations are needed in case of inherited thrombophilia. We analyzed two pediatric patient populations with AT deficiency, one in Hungary (n=32) and another in Serbia (n=19) (*Gindele et al. Thromb Res 2017; 160:119-128 and Kovac et al. Eur J Pediatr 2019;178:1471-1478).* Most of the children were of type IIHBS mutants (n=41) and the majority of children (n=31) were homozygous carriers of ATBp3. There were two peaks of age (0-1 years and 12-18 years) at the time of first thrombotic episode. All but one infant (i.e. 0-1 years) with thrombosis was ATBp3 homozygotes. Vascular anomaly was diagnosed in 2 children (v. cava inferior aplasia and hypoplasia of both iliacal veins and hypoplasia of v. cava inferior and v. iliaca communis). Ischemic stroke and myocardial infarction (MI) were also observed in type IIHBS AT deficient children. We concluded that type IIHBS AT deficiency; especially ATBp3 homozygosity is a strong risk factor for VTE and also for ATE in children.

We investigated the laboratory behavior of type IIHBS AT deficiency. AT activity was determined by three different heparin-cofactor anti-Xa-based amidolytic assays (our assay and two alternative commercially available functional assays). Our assay used as reference, since it showed 100% sensitivity to all AT deficiency types. Assay1 (Innovance AT, Siemens, Marburg, Germany) uses human, while assay2 (HemosIL AT, Instrumentation Laboratory, MA, USA) and our assay uses bovine FXa as substrates and they also differ in the chromogenic substrate type (Z-D-Leu-Gly-Arg-ANBA-methylamide-acetate in assay1, S-2765 (N-α-Z-D-Arg-Gly-Arg-pNA•2HCl) in assay2 and succinyl-Ile-Glu(γPip)Gly-Arg-paranitroaniline HCl substrate in our assay), final sample dilution (1:20 in assay1, 1:120 in assay2 and 1:50 in our assay), heparin concentration (1500 U/L in assay1, 3000 U/L in assay2 and 1000 U/L in our assay) and in the dilution buffer (Tris-HCl, pH 8 in assay1, sodium-chloride, pH 7.4 in assay2 and Tris-HCl, pH 8.4 in our assay). While the assays gave similar results in type IIRS and type IIPE patients heterogeneous results were observed in type IIHBS deficiency. While assay 1 and our assay gave low AT activity in all AT Padua I and Basel cases, assay 2 did not recognize these mutants showing normal AT activity for all patients. AT activity values were decreased in ATBp3 homozygotes with all assays; however, the results obtained by assay2 were significantly higher than those in the other tests, suggesting heterozygous state. The sensitivity of assay2 for ATBp3 heterozygosity was only 44%. It was suggested by these findings the substrate type (i.e. anti-FIIa or anti-FXa assay) is not the only factor that influences the sensitivity of functional AT assays, since all the investigated assays were anti-FXa based tests. We investigated therefore the effect of heparin concentration and pH of assay conditions on assay sensitivity by introducing

modifications in our assay (Figure 3). Upon increasing the heparin concentration in the assay all AT activity values increased and in one sample with AT Padua I it reached the lower limit of the reference interval. AT activity values further increased, reaching or exceeding the lower limit of the reference interval in 2 AT Basel and in 1 AT Padua I samples by changing the assay conditions to pH 7.4. When the heparin concentration of the original assay increased by 8-fold all AT Basel and Padua I samples gave normal AT activity results. AT activity values of ATBp3 samples did not increase further.

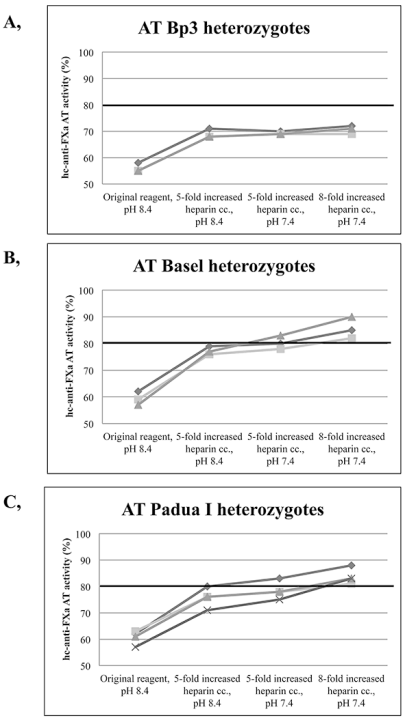

Figure 3. Effect of assay modifications on the AT activity values of AT Budapest 3 (A), AT Basel (B) and AT Padua I (C) heterozygote samples.
The effect of increased heparin concentration and lowered pH on AT activity values by modifying the original (reference) diagnostic assay is shown. The upper limit of the reference interval (80%) is highlighted with thick horizontal line.

Our results suggest that the high heparin concentration and perhaps the lower ionic strength are major factors that decrease the sensitivity of the assays to type IIHBS deficiency, especially to AT Basel and Padua I. Our results strengthen the hypothesis that type IIHBS deficiency is a heterogeneous group with different strength of heparin binding according to the specific mutations. This results in different behavior in the functional assays. Assay modifications, that were tested, had less effect on AT activity values of ATBp3 samples, which suggest more complex consequence of this mutation than being a heparin-binding defect. Based on our results it is to be noted, that type IIHBS AT deficiency may be under-diagnosed by some commercially available functional assays, which is of great importance from the point of view of routine laboratory protocols. Based on our experience with laboratory assays and genotype-phenotype correlations a novel laboratory protocol was recommended for AT deficiency diagnosis (*Bereczky et al. e-JIFCC 2016;27:130-146.)*.

We investigated the effect of ATBp3 mutation on thrombin generation by means of Innovance ETP (Siemens) on a BCS-XP coagulometer and expressed as endogenous thrombin potential (ETP). Our results showed that all carriers of *SERPINC1* mutations had significantly higher ETP than wild type individuals, however only a slight and non-significant difference of ETP was registered among type I, IIHBS heterozygous and homozygous samples, which was not concordant with the heterogeneous clinical phenotype. This suggests that additional factors may play a role by modifying the basal risk for the development of thrombosis in AT deficiency. (*Kovac et al. Thromb Res 2018;166:50-53.*)

An interesting co-inheritance of AT deficiency (p.Arg79His, AT Padua) with dysfibrinogenaemia (FGA p.Arg35His) was discovered in a family with thrombotic symptoms (*Gindele et al. Life 2021; in press*).

2, Investigation of the founder effect in ATBp3 mutation and determining its age and origin.

ATBp3 (p.Leu131Phe) was the most frequent mutation in our cohort of AT deficient patients and it was also a recurrent variant in our neighboring country, Serbia. There were some sporadic reports before our population-based study about this mutation suggesting its Central Eastern European accumulation and founder effect. By establishing the detection of different molecular markers (Alu 5, Alu8, D1S196, D1S218, the 5'length polymorphism, rs5877, rs5878, rs2227596, rs941989, rs2227612, rs1799876, rs677 and F13A1-STR as negative control) n=102 ATBp3 patients, n=200 healthy controls representing the general Hungarian population were investigated. It was demonstrated that in the case of all ATBp3 carriers the pathogenic „T" allele was associated with one haplotype (Table 1). The normal „C" allele was associated with different haplotypes both in ATBp3 carriers and controls. ATBp3 homozygous patients shared one distinct Alu5 and Alu8 repeat number variations $(ATT)_6$ and $(ATT)_{15}$, respectively. The founder effect of ATBp3 mutation was undoubtedly confirmed by us in the largest population in the literature using the highest number of genetic markers (*J Thromb Haemost, 2016;14:704-15*).

Table 1. Results of haplotype analysis in ATBp3 carriers and in the general population.

ATBp3 carriers (n=102)												General population (n=200)						
		rs5877	rs5878	5'LP	rs2227612	rs941989	rs2227596	rs1799876	rs677	Frequency			5'LP	rs2227612	rs941989	rs2227596	Frequency
c.391 „T allele"		A	A	S	A	G	A	T	G	0.592								
c.391 „C allele"	Haplotype 1	A	A	S	A	G	A	T	G	0.183		c.391 „C allele"	Haplotype 1	S	A	G	A	0.630
	Haplotype 2	G	G	L	A	A	A	C	G	0.083			Haplotype 2	L	A	A	A	0.104
	Haplotype 3	G	G	L	C	A	G	C	C	0.058			Haplotype 3	L	C	A	G	0.147
	Haplotype 4	G	G	L	C	A	G	T	C	0.025			Haplotype 4	S	A	A	A	0.077
	Haplotype 5	G	G	S	A	A	A	C	G	0.025								

*S, short, 32 bp; L, long, 108 bp

We then aimed to calculate the age and origin of ATBp3 and to explore whether the frequency of it is higher in the Roma population as compared to the general population from the corresponding geographical area. We investigated the Roma population, the

largest ethnic minority in Europe because this population has increased susceptibility to thrombotic diseases partly due to their unfavorable genetic load. Prevalence of ATBp3, investigated in large samples (n=1000 and 1185 for general Hungarian and Roma populations, respectively, recruited in the framework of the Hungarian General Practitioners' Morbidity Sentinel Stations Program, H-GPMSSP) was considerably high, almost 3%, among Roma and the founder effect was confirmed in their samples, while it was absent in the Hungarian general population.

For the determination of the age of ATBp3 genomic DNA from 36 unrelated index subjects with ATBp3 mutation and their family members out of our large AT deficient group were haplotyped for alleles at 8 STRs; 7 dinucleotide and 1 tetranucleotide repeats; heterozygosity >0.7, namely D1S212 (4.92 ΔcM) – D1S2659 (3.27 ΔcM) – D1S218 (0.73 ΔcM) – D1S2790 (1 ΔcM) – D1S1165 (2.43 ΔcM) – D1S2815 (2.53 ΔcM) – D1S196 (7.35 ΔcM) – D1S460 (54.8 ΔcM) flanking the disease locus. Distances of the markers from ATBp3 are given in the brackets (Figure 4). The fragments containing the STRs were amplified by PCR and the amplicons were tested for length polymorphism by capillary electrophoresis on an ABI3130 Genetic Analyzer (Thermo Fisher Scientific). Analysis of STR sequences was implemented by the GeneMapper v4.1 software (Life Technologies). Two hundred individuals out of the n=1000 Hungarian reference population as control subjects and n=94 individuals out of the n=1185 Roma reference samples were also tested for these STR markers.

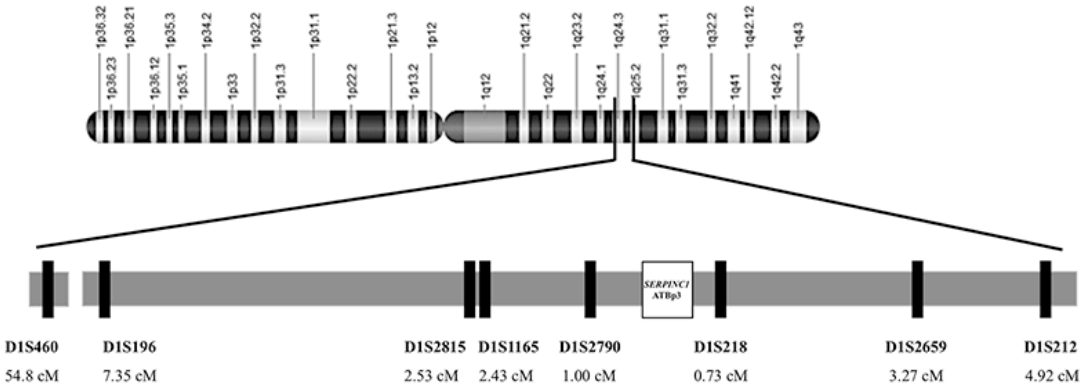

Figure 4. Genomic map of chromosome 1. Localization and position of SERPINC1 gene and the analyzed short tandem repeat markers on region 1q24-25.
Short tandem repeat markers are D1S460 (CA)n, D1S196 (AC)n, D1S2815 (CA)n, D1S1165(CTTT)n and D1S2790 (CA)n locate proximal to SERPINC1 and D1S218 (AC)n, D1S2659 (CA)n, and D1S212(CA)n locate distal to SERPINC1.

The age of an allele is the duration of time elapsed since it was created by a mutation. Age estimates can be made by different methods considering variations at marker loci and allele frequency. Linkage disequilibrium, LD index values were calculated and genetic distances were obtained from physical distances (Genome Reference Consortium Human Build 38) between STRs and *SERPINC1* by applying a conversion factor of 1.17 cM/Mb derived from the Marshfield map. The age of ATBp3

(in generations, g) was initially estimated by two moment methods. Besides simple parametric age estimators we reanalyzed LD data in a Bayesian perspective using the Markov chain Monte Carlo method implemented in the DMLE+ program, version 2.3 (available at http://www.dmle.org), and a second likelihood method, which estimates the distance (in generations) from probands sharing a common haplotype to the most recent common ancestor (MRCA) by the means of the ESTIAGE software. By investigating the n=36 unrelated ATBp3 mutants and their family members (n=70, altogether n=106) a fully conserved ancestral haplotype - D1S212: 20 – D1S2659: 11 – D1S218: 24/25 – D1S2790: 20 – D1S1165: 13 – D1S2815: 18 – D1S196: 12 – D1S460: 7 (where numbers after the markers represent the most frequent repeat number variations) was identified in 14 independent chromosomes. In addition, related haplotypes, likely derived from the ancestral one by either recombination or mutation at the flanking markers, were found in the remaining chromosomes. We analyzed the frequencies of repeat alleles associated with ATBp3 and compared them to the corresponding allele frequencies in 200 unrelated control Hungarian subjects recruited from the general Hungarian population who did not carry ATBp3 mutation. The most frequent haplotype in the Hungarian population for the investigated markers were as follows: D1S212: 20 – D1S2659: 15 – D1S218: 25 – D1S2790: 21 – D1S1165: 11 – D1S2815: 18 – D1S196: 12 – D1S460: 7. The mean±SD overall age estimate for the SERPINC1 c.391C>T mutation, based on the LD data for the 8 STRs, was 11.5±5.47 g according to the first moment method and it was 11.8±7.1 g according to the iterative procedure of the second one (Table 2). The Markov chain Monte Carlo method provided similar estimation of 13 g (95%-credible-set [CS]: 3–42 g) and the age estimation was 14 g (95%CS: 5–37 g) by the second likelihood method.

Table 2. Estimation of the age of the c.391C>T mutation in the *SERPINC1* gene by different methods.

Marker	Distance	Repeat number variatons	LD	MRCA age		Founder event of ATBp3 (date)	
	ΔcM		δ	*g*	*y*	Date	95%CS
D1S212	4.92	20	0.326				
D1S2659	3.27	11	0.628				
D1S218	0.73	24/25	0.945				
D1S2790	1.00	20	0.899	11.5±5.47	287±137	1703±137	NA
D1S1165	2.43	13	0.741				
D1S2815	2.53	18	0.731				
D1S196	7.35	12	0.470				
D1S460	54.8	7	0.086				
All haplotypes		DMLE+		13	325	1665	940-1915
All haplotypes		ESTIAGE		14	350	1640	1065-1865

NA, not applicable; CS, credible set (Bayesian analogue of confidence interval in classical frequentist statistics). LD, linkage disequilibrium between the allele and the *SERPINC1* c.391C>T mutation; MRCA, most recent common ancestor of the c.391C>T-mutation-bearing chromosomes, whose age is expressed in generations (*g*) and years (*y*), assuming a mean value of 25*y*/*g*; DMLE+, software implementing the Markov chain Monte Carlo algorithm to allow Bayesian estimation of the MRCA age; ESTIAGE, software implementing a likelihood-based method of inferring the MRCA age from multilocus haplotypes; Distance

(ΔcM, centiMorgan) is the genetic distance between the marker and the *SERPINC1* locus on chromosome 1. Repeat number variations represent the most frequent repeat numbers in homozygous ATBp3 probands. Historical date of the founder event that has likely increased the frequency of the c.391C>T mutation in the Hungarian population, based on the MRCA age and a mean date of birth for mutation's carriers equal to 1990.

Assuming an average of 25 years per generation and that the average birth year of the mutation carriers investigated is 1990, the present results suggest MRCA bearing the c.391C>T mutation back to middle of the XVII century (350-400 years ago). This dating points to the origin of the founder effect at a very turbulent period of the history of Hungary with settlement of different populations including Roma tribes. The estimated age of the *SERPINC1* c.391C>T mutation, the geographic distribution of families with ATBp3, and the history of the modern Hungarian population are consistent with the hypothesis that the mutation originated (or was originally introduced) and expanded in the later Ottoman period and Royal Hungary. The considerable carrier frequency (around 3%) in such a rare disease, that was found in the Roma general population and the confirmation of the founder effect in this population strengthens the hypothesis that the mutation is of Roma origin, or at least became more prevalent in that population. Based on our results it is recommended to include the investigation of ATBp3 AT deficiency as part of thrombosis risk-stratification in Roma individuals (*Bereczky et al. Front Cardiovasc Med 2021;7:617711*).

By using our experience in the investigation of founder mutations we successfully confirmed the presence of founder effect of a novel *ACVRL1* c.625+1G>C mutation in hereditary hemorrhagic telangiectasia (HHT) in collaboration with a study group working on Osler's disease (*Major et al. Clin Genet, 2016;90:466-467*). Then we started a systematic clinical genetic study concerning the genotype-phenotype associations in this disease and we introduced an algorithm for the stratified population screening; we called the attention to the importance of searching for HHT and performing genetic testing, especially in populations where founder mutations are present (*Major T et al. Pathol Oncol Res 2020;26:2783-2788, Major T et al. J Int Med Res 2019, Major T et al. Orv Hetil 2019;160:710-9.)*

3, Investigation of the molecular mechanisms by which ATBp3 leads to AT deficiency; detailed characterization of its heparin binding properties.

Consequences of ATBp3 mutation at a molecular level were investigated by in vitro biochemical methods and by in silico analysis. Before analyzing the differences between wild type and ATBp3 AT we characterized the mechanism of the allosteric activation of AT by means of advanced sampling simulations. Briefly, in order to investigate the earliest steps of conformational activation (ie. the early binding events of a pentasaccharide to AT), we performed molecular dynamics (MD) simulations using an "enhanced" sampling method, Gaussian Accelerated Molecular Dynamics (GAMD). This method provides highly enhanced sampling without pre-defined reaction coordinates and was used previously in drug binding studies. In our GAMD simulations, we have studied the binding of a pentasaccharide ligand to a non-activated AT conformation. Furthermore, we performed enhanced sampling MD simulations on two further model systems, one corresponding to an activated state of AT with a ligand, and one containing no pentasaccharide. We could observe the binding of the pentasaccharide ligand

idraparinux to a "non-activated" AT conformation in two independent 1 μs GAMD simulations, with low "root mean square deviations" (RMSD) of the ligand compared to an X-ray structure of activated AT. In both trajectories, subunit H of the pentasaccharide (the reducing end) reached its "final" position after subunit D (the nonreducing end). From the trajectories of our simulations, we could study the conformation changes of the hinge region, the C-terminal end of helix D and the reactive center loop. Our advanced sampling simulations confirmed the high stability of helix P even in the absence of a ligand. These results suggest a possible role of AT conformations with a "pre-formed" helix P in the heparin binding process. Our calculations revealed possible regions of AT that are likely involved in the propagation of allosteric signal from helix D (involved in heparin binding) to the binding exosite for coagulation factor Xa (*Balogh et al. J Biomol Struct Dyn 2020;38:4718-4732*).

As the affected amino acid in case of ATBp3 mutation is not involved directly in the binding of the high-affinity pentasaccharide unit, long molecular dynamics (MD) simulations were required to investigate the effects of the mutation on the binding. The simulations were performed using the advanced sampling method GAMD. The consequences of the ATBp3 mutation were investigated in both the high-affinity pentasaccharide bound and the not activated conformational state of the protein. We compared the results from the MD analysis to data obtained from wild type AT simulations. Two independent GAMD simulations were performed on the pentasaccharide-free, non-activated AT system. Our most important observations regarding this system are the increased fluctuation (RMSF) values for several regions of the protein, compared to the wild type AT simulations (Figure 5). Increased fluctuations can be observed both in parts of the protein close to the affected amino acid (residues 50-100), as well as in more distant regions (amino acids 320-330, 360-380, 420-430). These findings are consistent with a moderate decrease in the stability of the native conformation of the protein. From the AT-pentasaccharide complex simulations, we analyzed the binding position/conformation of the pentasaccharide, using root mean square deviations (RMSD) from the X-ray diffraction structure 1NQ9. We could observe increases in the RMSD values compared to equilibrium MD simulations in two of three independent GAMD simulations, indicating weaker binding of the pentasaccharide to the protein (Figure 6). To investigate the changes in the allosteric processes caused by the mutation, we also investigated the correlated motions. The calculated correlation matrices were different from those obtained for the WT protein, indicating changes in the allosteric pathways.

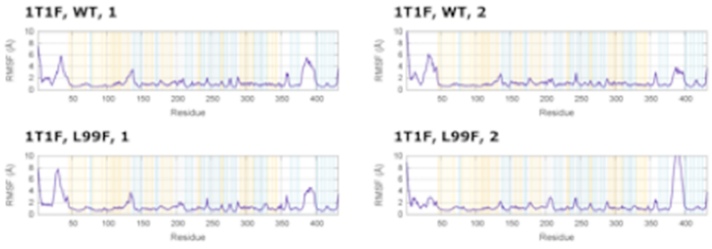

Figure 5. Root mean square fluctuations of the α-carbon atoms, from the simulations not containing a pentasaccharide ligand ("1T1F-based").
The background of the plots is colored by the secondary structure of the region (orange – α-helix, blue – β-sheet.)

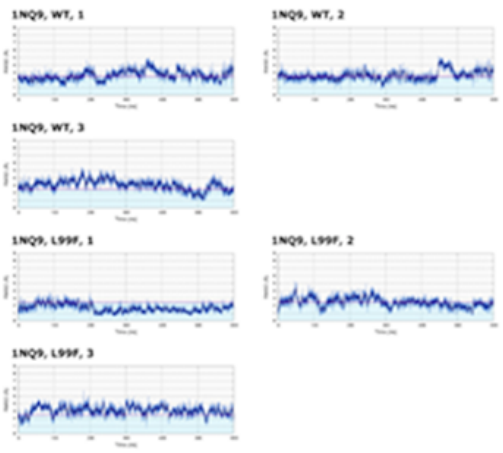

Figure 6. RMSD of the ring and interglycosidic atoms in the heparin pentasaccharide from wild type and ATBp3 AT-pentasaccharide system simulations, compared to the X-ray diffraction structure 1NQ9.

For the in vitro biochemical studies of ATBp3 the cDNA clone ORF-NM_000488_pcDNA3.1(+) wild type AT (WT) was purchased and ATBp3 mutant plasmid was created by QuickChange Site-Directed Mutagenesis (Agilent Technologies, Santa Clara, CA, USA) kit. Stable transfection of Human embryonic kidney (HEK-293) cells with huSER-PINC1_pcDNA3.1(+) WT and ATBp3 plasmids was performed with Lipofectamine®3000 Transfection Kit (Invitrogen). Geneticin® Selective Antibiotic (Gibco) was used as a selective agent. Media containing expressed WT and mutant AT proteins were harvested and concentrated on an Amicon® Ultra 30 kDa (Merck Millipore, Burlington, USA) column for further investigations. AT proteins by affinity-chromatography using Goat anti-human Antithrombin IgG (Affinity Biologicals, Ancaster, Canada) that was covalently coupled to Sepharose 4B gel. The concentration of purified AT proteins was determined by immunonephelometry (Siemens). Crossed immunoelectrophoresis (CIE) and surface plasmon resonance (SPR) assays were performed, the latter on a Biacore 3000 instrument (GE Healthcare, Uppsala, Sweden) by using heparin SPR sensorchip (Heparin Approx. 50 nm hydrogel chip, XanTec bioanalytics GmbH, Dusseldorf, Germany). Wild type and mutant AT, diluted in running buffer (HEPES 10 mM, NaCl 150 mM, EDTA 3 mM, surfactant 0.005% [v/v], pH 8.4), were injected into the microflow cell in 6 different concentrations (50, 100, 150, 300, 500, 750 nM) and kinetic parameters were calculated by the BIAevaluation software (GE Healthcare, Uppsala, Sweden). NanoDSF is a differential scanning fluorimetry method used for accurate analysis of protein folding and stability. It measures the intrinsic tryptophan or tyrosine fluorescence for the analysis. During unfolding of proteins tryptophan becomes hydrated and its fluorescence intensity maximum is shifted from 330 nm to 350 nm. The thermal stability of a protein can be described by the thermal unfolding transition midpoint (T_m) at which half of the protein population is unfolded. Thermal stability is also characterized by the onset temperature (T_{onset}) of the

denaturation. The dual wavelength system of the Prometheus NT.48 (NanoTemper Technologies GmbH, Munich, Germany) was used to characterize the thermal unfolding processes of wild type and ATBp3 AT proteins. Our major findings were as follows: In the case of ATBp3 homozygote plasma only heparin low affinity AT could be visualized by CE. In the case of the WT AT the T_{onset} and T_m values were 46.2±1.3°C and 57.6±0.1°C, respectively, while for the mutant AT the T_{onset} was 42.7±1.47°C and the T_m was 57.1±0.03°C. Both T_m (p=0.0031) and T_{onset} (p=0.0371) values were significantly lower in case of the ATBp3 mutant compared to WT AT indicating a lower thermostability for the mutant protein. In SPR experiments as it was expected, a strong AT-heparin binding was observed in the presence of the wild type AT (K_D = 6.4 x 10^{-10} M, K_A = 2.2 x 10^9 1/M). The association rate constant (k_a) was high (k_a = 1.37 x 10^7 1/Ms). These data suggest that the formation of the AT-heparin complex occurs rapidly in case of wild type AT. As compared to the data obtained for the wild type protein, ATBp3 appeared to exhibit a significantly weaker interaction with heparin, with a slower association rate (K_D = 2.15 x 10^{-8} M, K_A = 1.62 x 10^8 1/M, k_a = 3.25 x 10^5 1/Ms). The dissociation rate constant for ATBp3 mutant was k_d = 2.47 x 10^{-3} 1/s and it did not differ significantly from that of wild type protein (k_d = 6.75 x 10^{-3} 1/s) (Figure 7).

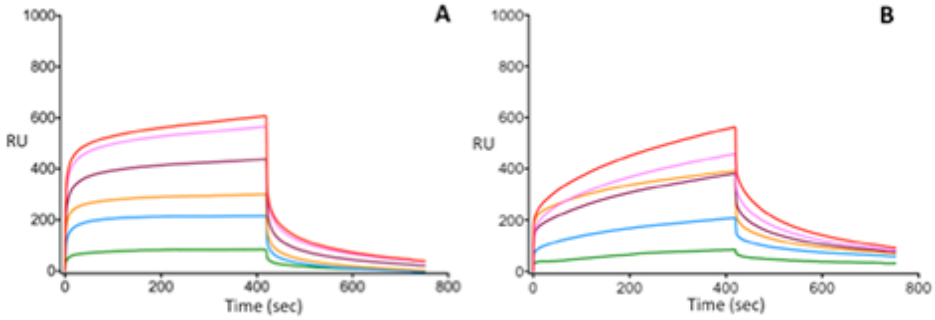

Figure 7. Analysis of AT-heparin interaction of wild type (A) and mutant (B) AT by Surface Plasmon Resonance method.

AT forms at six different concentrations (1, 3, 5, 7, 9 and 11 nM from bottom to top curves in the pictures) were injected into the microflow cells on the same chip. SPR sensorgrams demonstrate the binding of the given AT to heparin at different concentrations. RU, response unit

As a conclusion form the biochemical and in silico analyses ATBp3 showed a two-magnitude weaker heparin-interaction in SPR studies and the allosteric activation of ATBp3 was affected, moreover the increased fluctuation in multiple regions of the molecule suggested that this variant had a destabilizing effect. These findings together with the decreased thermostability of ATBp3 suggest the presence of a quantitative component in the pathogenicity of this mutation (*Gindele et al. Biomolecules, 2021, accepted with revision*).

4, Characterization of novel mutations of the natural anticoagulants.

At present data of n=446 AT deficient patients, n=173 PC deficients and n=72 PS deficient patients, all confirmed by genetic studies are available. In AT deficiency we identified n=18 novel mutations out of the 39 (Figure 8), while in PC and PS deficiencies n=20 (out of n=58) and n=14 (out of n=33) novel mutations were described in *PROC* and *PROS1* genes, respectively.

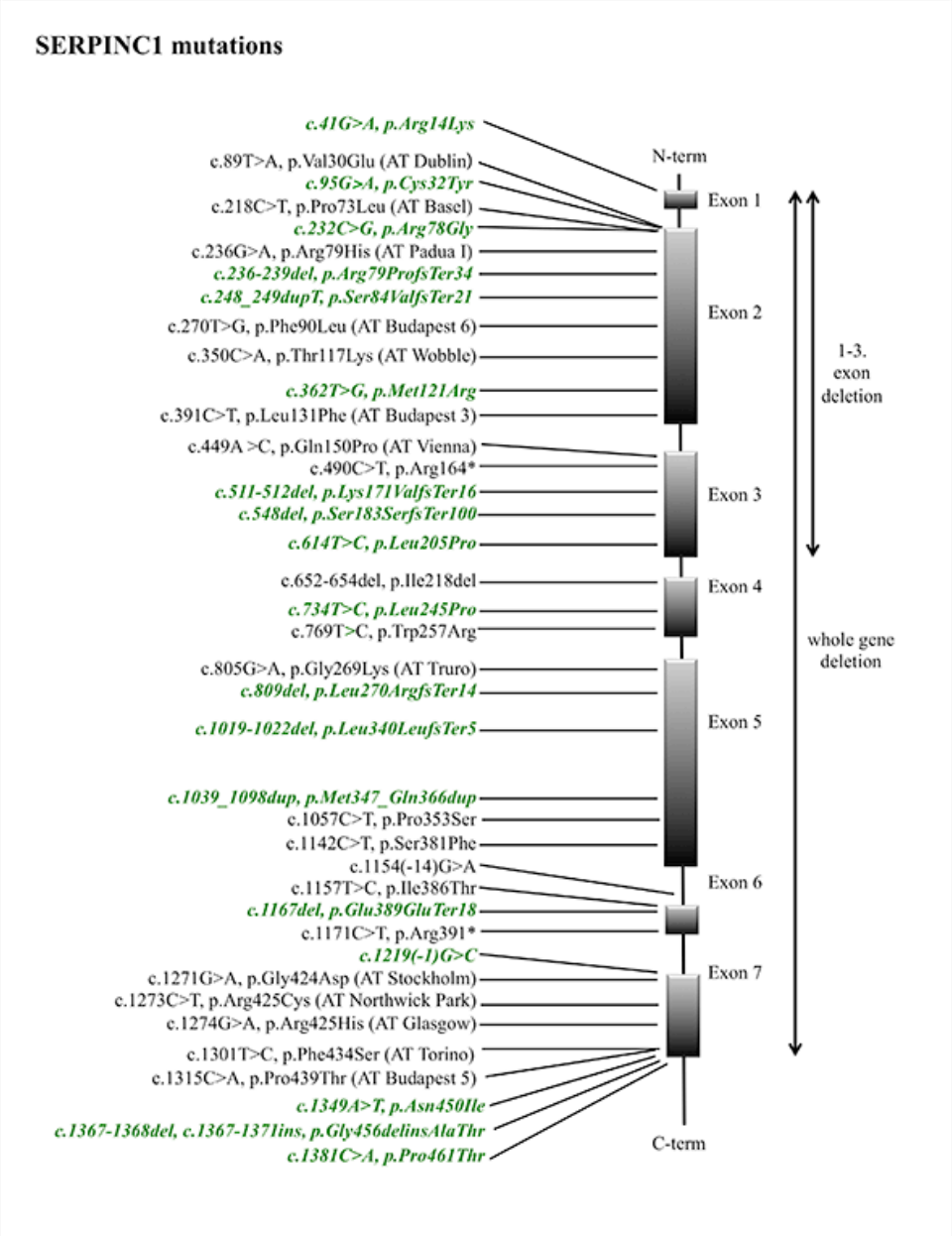

Figure 8. *SERPINC1* mutations detected during the study period. Novel mutations are labeled in green.

The pathogenicity of the novel mutations were evaluated by different prediction tools, PolyPhen2, MutPred2, PhD-SNP, Mutation Taster and SIFT and in vitro studies were carried out in transiently expressed mutant proteins. We detected the expressed mutants by ELISA and immunoblotting in cell lysates and media. Depending on the results, if secretion abnormality was suspected, further examinations were pulse-chase analysis, double immunofluorescent labeling of the mutant protein and different cell organelles and visualization by confocal laser scanning microscopy, and we performed specific mRNA quantitation and examination of anti-FXa activity in case of *SERPINC1* mutants. Functional studies, if qualitative disorder was suspected were also executed in *PROC* and *PROS1* mutants. Until recently, we could draw conclusions for 10 *SERPINC1*, 4 *PROS1*

and for almost all *PROC* variants. Among *SERPINC1* mutations p.Leu205Pro was investigated most extensively, since the clinical phenotype-molecular phenotype-genotype associations could be analysed in most details thank to the largest number of patients (a large family, with a total number of 31 in four-generations) carried this mutation (*Selmeczi et al. Thromb Res 2017;158:1-7*). While wild type AT appeared as a clear band in the conditioned media of HEK cells at 58 kDa, only a faint band of Pro205 AT could be visualized. Both WT and mutant AT were demonstrated as equally intense bands in the cell lysates. Secretion defect of mutant AT was confirmed by ELISA measurements in cell lysates and media of transfected cells and pulse-chase analysis suggested intracellular accumulation and degradation. Pro205 AT occupied a relatively high fraction of trans-Golgi and 26S proteasome as it was demonstrated by the significantly higher PPI1 values and Pearson's correlation coefficients. The median of correlation coefficient was 0.48 for Pro205 AT and trans-Golgi suggesting moderate degree of co-localization, while it was even higher, 0.71 for Pro205AT and 26S proteasome suggesting strong degree of co-localization with this cell-organelle. Results of molecular modeling studies suggested misfolding and structural instability of the mutant AT (Figure 9). The average specific activity (ie. the activity related to one mg AT protein) obtained in independent experiments of Pro205 was 3.94±0.95 U/mg, while it was 7.79±2.10 U/mg in the case of the WT AT suggesting complex consequences of the mutation (ie. secretion defect due to structural abnormality and functional alteration).

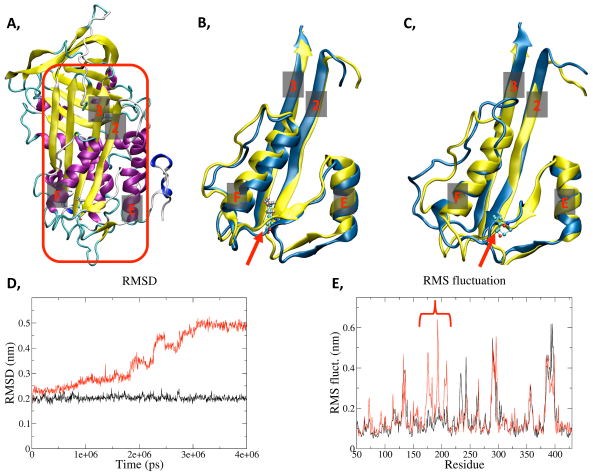

Figure 9. Graphical representation of the effect of p.Leu205Pro mutation on the structure of antithrombin.

A, Cartoon representation of AT structure. Leu205 residue is shown by sphere model. The α-helical and β-string structure elements are depicted in purple and yellow, respectively. The location of 167-257 residues which includes the Leu205 residue and whose properties are examined in details are inside the red rounded rectangle. The 2nd and 3rd strings of β –sheet A are numbered as "2" and "3". Two helices, E and F can be found in the selected region.

The superposition of the snapshots from the first and last frame of the 4 μs simulation carried out for the wild type (B) and Pro205 (C) proteins. Only residues between 167-257 are shown. Cartoons corresponding to the first and the last frame are colored in yellow and blue, respectively. The residues Leu205 (B) and Pro205 (C) are shown by a sphere representation while their positions are marked by red arrows. D, Root-mean-square deviation from the starting structure during the productive dynamics simulations for both the wild type (black line) and the Pro205 (red line) mutant proteins. Only the residues between 167-257 were

considered in the calculations. E, Root-mean-square fluctuations for each residue calculated for both the wild type and the Pro205 mutant AT. Black color indicates the wild type AT while the corresponding values for the mutant protein are shown in red color. The region demonstrated significantly increased fluctuation compared to the wild type protein is marked by brace. The residue numbering on this figure corresponds to the X-ray structure file (i.e. signal peptide residues are not counted).

Among other SERPINC1 mutants decreased amount of mRNA was demonstrated in the transfected HEK cells of p.Asn450Ile, p.Gly456delinsAla_Thr and p.Leu270ArgfsX13 suggesting decreased synthesis of mutant AT proteins. These findings were confirmed by Western blot and Pulse-chase analysis (disappearance of the band corresponding to mutant AT from the cell lysates between 120 and 360 min) suggested rapid degradation in case of the former two mutants, while p.Leu270ArgfsX13 was absolutely undetectable even within the transfected cells. Defective synthesis was also confirmed in case of p.Cys32Tyr. Besides the above-mentioned quantitative defects functional variants were also detected. The p.Pro461Thr, p.Arg14Lys, p.Arg78Gly, p.Met121Arg and p.Leu245Pro mutations produced in the same amount as the wild type or even in higher concentration. Among them the secretion was decreased for p.Arg14Lys, p.Met121Arg and p.Leu245Pro together with decreased heparin-cofactor and progressive anti-FXa activity suggesting complex phenotype. In case of p.Pro461Thr and p.Arg78Gly no secretion defect was observed, instead severe functional defect was shown in both heparin-cofactor and progressive anti-FXa assays. (p.Pro461Thr: 25-30%, p.Arg78Gly: 1-5% activity of wild type).

Based on our results of in silico and in vitro biochemical studies (including phospholipid dependent and amidolytic functional studies) *PROC* mutants could be classified into four major groups. The first group includes mutants with unequivocally confirmed quantitative deficiency with decreased synthesis or secretion and molecular instability (p.Cys122Phe, p.Arg272Cys, p.Gly393Arg, p.Gly109Cys, p.Cys160Arg, p.Ala309Pro and p.Asp401Asn). The second group involves mutations with complex – secretion defect with phospholipid dependent functional defect - consequences (p.Arg57Trp, p.Arg57Gln, p.Glu61Lys, p.Arg129His, p.Ala333Asp). We classified functional defects without secretion disorders into the third group (p.Arg64Ser, p.Lys70Glu). Finally, when pathogenecity could not be confirmed in vitro we considered the mutations as likely benign (p.Ser30Arg, p.Arg123Ser and p.Ala408Thr). Further studies are needed to clarify the consequences of p.Thr110Arg, p.Ser223Asn and p.Ala333Thr.

Based on our studies pathogenicity of p.Thr98Ser, p.Asn168Ser, p.Ile395Val and p.Phe577Cys missense mutations in *PROS1* could not be confirmed, which was concordant with in silico predictions.

II. Determination of the role of the natural anticoagulants and polymorphisms in arterial thrombotic diseases

Our aim was to investigate the role of the deficiencies of the natural anticoagulants and the presence of different polymorphisms in arterial diseases. We also focused on the investigation of the impact of *SERPINC1* mutations, especially ATBp3 in different types of thrombosis. During this project we recruited different groups of patients (see below). We aimed to investigate the association of type IIHBS mutations, including the prevalent ATBp3, with VTE and ATE in well-defined populations to see whether it is relevant to

give a recommendation for more extensive testing for AT deficiency in certain populations. In details:

1, Association of AT Budapest 3 with cardiovascular diseases.

To investigate the association of AT IIHBS deficiency and thrombotic diseases different patients' groups were collected.

First, n=243 non-related genetically confirmed type IIHBS AT deficient patients (index patients) diagnosed at our center and their affected family members (total n=328), were involved. Inclusion criteria were low AT levels measured by anti-FXa heparin cofactor AT activity assay (hc-anti-FXa) and the confirmed type IIHBS mutation in the genetic test.

A second group including young adults with ST-elevation MI in their case histories below the age of 40 years was collected (n=119, median age 36 years, male/female 79%/21%) in order to investigate the association of hemostasis alterations with MI in this young age group, where the prevalence of occlusive arterial diseases was low. The diagnosis of MI based on the current guideline for universal definition of MI based on the biomarker detection plus the presence of clinical symptoms or ECG changes characteristics for myocardial ischemia or identification of coronary thrombus. Age-matched clinical control (CC) individuals (n=101, median age 36 years, male/female 59%/41%) were also recruited, who had undergone coronary angiography but no coronary artery disease has been revealed and no MI was recorded in their case histories. Indication of coronary angiography for them was the clinical suspicion for stable angina, as they had at least one positive non-invasive test for assessment of myocardial ischemia. This group was completed with samples required from an Italian cardiovascular study group including n=300 patients suffered from myocardial infarction.

A group consisting of consecutive, non-related patients with VTE in their case histories below the age of 40 was also investigated (n=110, median age 31 years, male/female 52%/48%). Thrombosis was diagnosed and categorized into spontaneous and provoked according to guidance of the International Society of Thrombosis and Haemostasis. Patient clinical, laboratory and genetic data were recorded in a database for further evaluation.

Roma individuals (n=402, median age 44 years, range 18-77, male/female 26.6%/73.4%) from the corresponding geographical area as the general Roma population (see I/2) were also recruited. The rationale of involving Roma individuals in the cardiovascular study was the surprisingly high frequency and the founder effect of ATBp3 mutation in the general Roma population.

Fasting blood samples were collected from all recruited individuals into 0.109 mol/L citrate vacutainer tubes (Beckton Dickinson, Franklin Lakes, NJ, USA) at least three months after the acute thrombotic episode or coronarography (if relevant) and stored at -80°C until use. Native blood samples were also collected and stored at -80°C. For diagnosing AT deficiency heparin cofactor (hc-anti-FXa) and progressive (p-anti-FXa) AT activity were measured (Labexpert Antithrombin H+P, Labexpert Ltd, Debrecen, Hungary, reference intervals 80-120% and 82-118%, respectively) on a Siemens BCS-XP coagulometer. AT antigen was measured by immunonephelometry (Siemens, N Antiserum to Human Antithrombin III, Marburg, Germany; reference interval 0.19-0.31 g/L). Protein C activity and free protein S antigen were measured by commercially available assays from Siemens (PC chromogenic and Innovance free PS

antigen). Fibrinogen was measured by the Clauss-method, measurement of other plasma or serum parameters was executed by routine methods using Roche reagents and instruments (Roche Diagnostics GmbH, Mannheim, Germany). DNA was isolated and ATBp3 mutation, FVL and the prothrombin 20210G>A polymorphisms were determined according to protocols developed in our laboratory on Roche LightCycler 480 instrument by using real-time PCR and melting curve analysis. The presence of different polymorphisms of the natural anticoagulants and polymorphisms of coagulation FXIII were also detected (see later).

While no ATBp3 was detected within the general Hungarian group (in our previous studies), the carrier frequency of ATBp3 was high, 2.74% in the Roma group. In this group ten heterozygotes (age range 24-60 years) and one homozygote (age 28 years) were registered. None of these patients have suffered VTE, as yet, however two of them had MI in their case histories. As FVL is also prevalent in the Roma population, the chance of having combined thrombophilia by carrying both FVL and ATBp3 is not negligible. Based on our results it is recommended to include the investigation of ATBp3 AT deficiency as part of thrombosis risk-stratification in Roma individuals.

Within our large cohort of AT deficient patients (n=435) the ratio of type IIHBS AT deficiency was extremely high; it was 75.4% (n=328 type IIHBS AT deficient patients, including n=19 AT Basel, n=30 AT Padua and n=279 ATBp3 individuals). The prevalence of thrombotic events, as expected, was significantly higher in the group of ATBp3 homozygotes as compared to any other groups. VT events (VTE) were registered in almost all patients with ATBp3 homozygosity (93%), while the frequency of VTE was below 50% in other groups. Clinical phenotype of ATBp3 homozygosity seemed severe enough not to be influenced by the presence or absence of a heterozygous FVL as clinical presentation of thrombosis in terms of the number of thrombotic episodes and the age at first symptoms were similar in patients with FVL and in wild type patients. In the group of ATBp3 heterozygotes carriership of FVL may shift the age at the first thrombotic episode to a lower range and it may have an impact on the severity. The number of ATE was much less than that of VTE, however it was not negligible. AT Basel patients showed a higher frequency of ATE, as compared to others; four patients out of the 9 suffered from ATE without having VTE in their case histories and in two of them the ATE was recurrent. They were all young at their first ATE. Among ATBp3 heterozygotes n=10 patients were registered with ATE. They were also young, the eldest patient was 48 years old at the time of MI.

Concerning classical thrombophilia risk factors almost 10% of MI patients were carriers of the FVL. While no protein C or protein S deficiency were found among these patients, there were three young MI patients with type IIHBS AT deficiency in our study group. Two of them were heterozygous carriers of the ATBp3 mutation, while one patient was a heterozygous carrier of the AT Basel mutation; all patients were males. There were no AT deficient individuals in the CC group. We also did not detect ATBp3 in the Italian MI group. As a comparison to our young MI patients, we investigated consecutive patients suffered from VTE below the age of 40 (n=110) recruited from our large cohort of four hundred VTE patients. There were huge differences in the prevalence of classical cardiovascular risk factors between VTE and MI groups. Among classical thrombophilia risk factors the allele frequency of FVL was significantly higher in the VTE group (more than 45% of the patients were carriers) and not only heterozygotes but

also homozygotes were found. The frequency of FII20210A carriers was only slightly higher in the VT group. Type IIHBS deficiency was registered in two VTE patients (both ATBp3 heterozygotes). In conclusion, the presence of type IIHBS AT deficiency (especially upon considering AT deficiency as a rare disease) is not negligible in young individuals suffering from any types of thrombosis and searching for AT Basel or ATBp3 in such selected populations, especially, in regions, where these mutations are prevalent, may be beneficial (*Bereczky et al. Front Cardiovasc Med 2021; 7:617711)*.

2, **Immunoassay development for the determination of β-antithrombin in human samples**

Our aim was to develop a sandwich-type immunoassay which uses a β-antithrombin-specific monoclonal capture antibody and a second labeled monoclonal antibody that recognizes both α and β isoforms of antithrombin.

In the first step we generated monoclonal antibodies against the synthetic peptide Ac-Leu-Tyr-Arg-Lys-Ala-**Asn**-Lys-Ser-Ser-Lys-Leu-Cys-$CONH_2$, which correspond to the amino acid sequence from Leu130 to Leu140 in AT. This peptide contains the Asn135 glycosylation site of AT without glycosylation, thus it corresponds to β-AT. Unfortunately none of the generated antibodies reacted with native β-AT despite of the high reactivity to the synthetic peptide. Therefore in the second step we prepared β-AT from pooled human plasma by heparin affinity chromatography and used the native protein to immunize mice. In this step we isolated antibodies that equally recognized α- and β-AT. These antibodies will be used as labeling antibodies in the immunoassay. However, no antibody specific for native β-AT has been found. In the next period computer simulation experiments were performed to design a cylic peptide with a 3-dimensional structure similar to that of the corresponding region in the native β-AT. The Tyr-Arg-Lys-Ala-Asn-Lys-Ser-Ser-Lys-Cys cyclic peptide was synthesized and conjugated to Keyhole Limpet Hemocyanin (KLH) and bovine serum albumin (BSA) through the SH group of cysteine and used for immunization and for testing antibody production, respectively. One of the generated cyclic peptide specific antibodies reacted also with native β-AT but not with α-AT. As all critical components of the immunoassay are now available, the development of the immunoassay for clinical use is under progress.

3, Effects of *SERPINC1, PROC, PROS1* and *EPCR* polymorphisms on the risk of VTE and ATE in young individuals.

Multiplex PCR followed by primer extension assay and fluorescently labeled ddNTP for detection by fragment analysis on a 3130 Genetic Analyzer was established to detect 12 SNP's simultaneously, as follows, PROC rs1799809 (IVS1-1641A>G), rs1799808 (IVS1-1654C>T), rs1799810 (IVS1-1476A>T), rs2069928 (IVS7+111G>T) and rs1401296 (3'UTR C>T); PROCR rs867186 (p.Ser219Gly), rs6088735 (5'UTR C>T) and rs8119351 (5'UTR G>A), SERPINC1 rs2227589 (IVS1+141G>A) and rs121909548 (p.Ala384Ser), PROS1 rs8178649 (IVS11+54T>C) and rs121918472 (p.Ser501Pro). First, we investigated the associations of these polymorphisms with the plasma levels of natural anticoagulants in n=358 healthy individuals recruited for the study. Protocol of sampling, storage and laboratory testing of AT, PC and PS was the same as for the study described in section II/1 above. The minor allele frequency values, which we detected in our study population, were comparable to the Caucasian population values (data obtained from the 1000 Genomes project) and they were in Hardy-Weinberg

equilibrium. AT Cambridge (rs121909548) was absent in our population. The allele frequencies of the other examined polymorphisms were as follows: *PROC* IVS1-1476 A>T (41%), *PROC* 3' T>C (34%), *PROCR* p.Ser219Gly (11%), *PROCR* 5' C>T (23%), *PROCR* 5' G>A (10%), *SERPINC1* IVS1+141 C>T (12%), *PROS1 IVS11+54* T>C (19%) and *PROS1* p.Ser501Pro Heerlen T>C (0.3%). Among *PROC* SNP's *PROC* IVS1-1641 A>G and IVS1-1476 A>T decreased PC activity significantly, when wild type and homozygous individuals were compared. No other *PROC* SNP's influenced PC activity. Among *PROCR* SNP's p.Ser219Gly and 5' G>A polymorphisms increased PC activity significantly both in the dominant and recessive models, while 5' C>T had the opposite effect, however it was significant only in the recessive model. By investigating the combined effect of *PROC* polymorphisms individuals who were carriers of *PROC* IVS1-1641 A>G and *PROC* IVS1-1476 A>T had the lowest, while those who were carriers of *PROC* IVS1-1641 A>G and *PROC* IVS1-1654 C>T had the highest PC levels. In case of *PROCR* polymorphisms the double carriers of *PROCR* p.Ser219Gly A>G and *PROCR* 5' G>A, who were wild type for *PROCR* 5' C>T had the highest PC levels. We did not find any differences in the adjusted levels of AT among individuals with different *SERPINC1* IVS1+141G>A genotypes. Similarly, *PROS1* IVS11+54 T>C polymorphism was without effect on adjusted PS levels. Carriers of PS Heerlen (PROS1 p.Ser501Pro) n=2 had significantly lower PS levels than those who were wild types (*Miklós et al. Clin Chem Lab Med 2016;54*:eA157-211).

After investigating healthy individuals we analysed the effects of these polymorphisms in young patients with ATE and VTE. General description of recruitment and sampling and laboratory protocols is provided in section II/1. Clinical characteristics of the different patients' groups are given in Table 2.

Table 2. Cinical characteristics of the study groups.

Clinical characteristics	healthy population (n=356)	VTE (n=114)	VTE control (n=277)	MI (n=78)	MI control (n=72)
Female (%)	60.4	47.4*	59.7	23.1	36.1
OAC (among females in pre-menopause) (%)	15.4	33.0*	16.0	NA	NA
Age (median and range, year)	36 (18-85)	40 (19-49)*	31 (18-49)	36 (24-40)	36 (26-40)
BMI (median and range, kg/m^2)	24.8 (16.3-41.4)	28.6 (19.0-52.7)*	24.2 (16.3-41.4)	28.0 (17.0-40.0)	28.0 (19.0-45.0)
DM (%)	0.8	7.1*	0	14.1	12.5
Hypertension %	17.4	9.6	12.2	43.6	50.0
Active smokers %	26.2	15.3	26.3	60.3§	22.2
Ex-smokers %	11.4	18.0	9.5	33.3§	20.8
Factor V Leiden mutation %	8.2	42.1*	8.3	10.3	9.7
Prothrombin 20210 G>A mutation %	3.4	7.0	2.9	2.6	1.4
VKA/NOAC/LMWH/TAG %	0	69.9/17.7/8.0/0	0	15.4/0/0/82.1	24.3/0/0/40.0

*p<0.05 (VTE versus VTE control); §p<0.05 (MI versus MI control); OAC, oral anticoncipient; DM, diabetes mellitus; VKA, vitamin K antagonist; TAG, antplatelet therapy

PROS1 IVS11+54T>C and *SERPINC1* IVS1+141G>A did not influence PS and AT levels and thrombotic risk. The rs1401296 (*PROC* 3' T>C) increased the risk of VTE by 2.5-fold (p=0.009) and in the contrary, rs867186 (*PROCR* p.Ser219Gly) was protective against VTE in FV Leiden negative patients (OR 0.24, p=0.026) and against

MI (OR 0.13, p=0.040). Elevated PC level seemed to be protective against VTE (Table 3).

Table 3. Effect of *PROC* and *PROCR* polymorphisms on the risk of VTE and MI.

Study group	predictor	OR (95%CI)
VTE vs. VTE control	FV Leiden	8.18 (4.39-15.24)
	BMI>30 kg/m2	4.46 (2.35-8.46)
	PC activity>130%	0.07 (0.01-0.53)
VTE (WT for FV Leiden)	*PROC* 3' T>C	2.59 (1.26-5.31)
	PROCR p.Ser219Gly	0.24 (0.07-0.84)
MI vs. MI control	smoking	25.8 (5.2-127.3)
	hyperlipidemia	15.5 (4.3-55.1)
	PROCR p.Ser219Gly	0.09 (0.01-0.49)

WT, wild type; OR was adjusted for FV Leiden and high BMI in the case of VTE and for smoking and hyperlipidemia in the case of MI when analyzed the effects of the SNPs. Only significant associations are shown.

Our observations suggest that PC levels and polymorphisms, that influence PC level may play a role not only in venous but also in arterial thrombosis, which is worthy of further investigations (*Miklós et al. Res Pract Thromb Haemost 2018;2:178*). To further investigate the role of these SNP's in arterial diseases a global hemostasis assay, which measures the amount of generated thrombin, was performed. PC levels and SNP's were correlated with the ETP (endogenous thrombin potential), maximum thrombin concentration and the lag phase of thrombin generation using Innovance ETP kit on BCS-XP coagulometer. PC showed a positive significant correlation with ETP and maximum thrombin concentration (Spearman's r 0.33 and 0.43, respectively, $p<0.001$) in MI patients, while there was no correlation with the lag phase of thrombin generation. These findings suggest that in the presence of higher potential to form thrombin the rate of PC synthesis is elevated in order to compensate the pro-coagulant mechanisms. The PC increasing effect of p.Ser219Gly was demonstrated even after adjustment to ETP and maximum thrombin concentration. The strong, positive correlation of thrombin generation parameters with BMI, oral contraceptive use and with the prothrombin 20210G/A polymorphism strengthened their role as thrombosis risk factors in our population. Based on our research and experience in the field, we were invited to write a comprehensive review in which we summarized the results of clinical studies concerning the association between MI risk and the deficiencies of the natural anticoagulants (*Bereczky Z et al. Kardiologia Polska 2019;77:419-29*).

We were invited into an international collaborative study group consisting of seven centers in five countries, Japan, South Korea, Singapore, Hungary, and Brazil to assess the worldwide distribution of three gene polymorphisms previously identified as

genetic risk factors among East Asian subpopulations, protein S (PS) Tokushima (p.Lys196Glu), protein C (PC) p.Arg189Trp, and PC p.Lys193del in a total of 2,850 unrelated individuals (1,061 VTE patients and 1,789 controls). The three variants showed different distribution worldwide and their were absent in the Caucasian population as represented by our recruited patients (*Tsuda et al. Res Pract Thromb Haemost 2020;4:1295-1300*).

4, Investigation of the role of coagulation FXIII-B subunit polymorphisms in VTE and ATE.

The common polymorphism of coagulation FXIII-A subunit (p.Val34Leu) was investigated extensively in VTE and ATE previously by us and by others, however we have much less data on the B-subunit polymorphisms. By investigating our recruited VTE and ATE patients for FXIII-B p.His95Arg (rs6003) and the IntronK c.1952+144C>G (rs12134960) polymorphisms we could draw interesting conclusions on the role of these variants in cardiovascular diseases of young individuals. The Intron K polymorphism significantly decreased FXIII levels in VTE patients, however it was without an effect on the risk of thrombosis suggesting its limited role in venous thrombotic events (*Mezei et al. Thromb Res 2017;158:93-97*). The results were more interesting in young individuals with MI. FXIII activity, FXIII-A_2B_2 and FXIII-B concentrations were significantly elevated in MI; Arg95 elevated, while Intron K "G" allele decreased FXIII levels. Smoking had an independent increasing effect on FXIII levels. The presence of IK "G" allele significantly decreased the risk of MI in patients with elevated fibrinogen. Among the investigated factors smoking and Intron K polymorphism had the most powerful effect on FXIII levels and the risk of MI in the young. We suggested that the effect of smoking on coronary thrombus formation may be at least partially attributed to its FXIII increasing effect (*Balogh et al. Mol Cell Biochem 2018;448:199-209*).

III. Investigation of novel aspects of the natural anticoagulants in coronary thrombus

Our aims were to better characterize the elements of coronary thrombi focusing on the relations of activated protein C (APC) to cells involved in thrombus formation and to the elements of neutrophil extracellular traps (NET). We observed if differences could be demonstrated in this aspect according to the age of the thrombi.

We collected coronary thrombi by manual thrombectomy aspiration device from n=167 patients (median age 59 years, range 30-86 years; 29% female, 71% male) underwent primary coronary intervention and thrombus aspiration due to the symptoms of acute MI. Among clinical characteristics the pain-to-ballon time was the most important from the point of view of the study, since it is expected to correlate with the age of the thrombus. Median pain-to-ballon time was 8 hours, the lowest value was 2 hours and the highest was 168 hours. Median weight of thrombi after aspiration was 20.85 mg, however they were rather heterogeneous in size (3.8-494.7 mg) and also in their macroscopic structure.

One part of the thrombus was fixed and embedded into paraffin. This was used for standard histomorphological analysis by which thrombi were chategorized into fresh, organizing (lytic) and organized. Another part of the thrombus immediately after

aspirating was deep frozened in liquid nitrogen until immunofluorescent staining. We established the protocols for multiple immunofluorescent staining and confocal laser scanning microscopy analysis. The staining circumstances were optimized for anti-Human Protein C, Anti-Histone H3 (citrulline R2 + R8 + R17), Alexa Fluor® 647 anti-human CD66b Antibody and their corresponding secondary antibodies and for SytoxGreen. After optimization of the multiple immunofluorescent staining protocols and establishment of the computerized analysis the thrombi were stained using following antibodies: Monoclonal Mouse anti-Human Protein C, and Dylight 488 Anti-Mouse IgG; Polyclonal Rabbit Anti-Histone H3 and Goat anti-Rabbit IgG-Alexa Fluor 568; monoclonal Mouse anti-human CD66b conjugated with Alexa Fluor® 647 (staining with Monoclonal Mouse anti-human CD68 conjugated with Alexa Fluor® 647 and Monoclonal mouse FITC-alpha2PI, in-house developed were also optimized). These sections were counterstained with DAPI and coversliped with Hydromount water-based mounting medium. For multiple immunofluorescent stainings we selected n=24 thrombi in which the age was unequivocally determined by immunohistochemistry. We stained n=8 thrombi in each category (multiple sections were prepared and investigated for each thrombus). Images were acquired by Olympus FluoView 3000 confocal microscope and the so-called multi-area time-lapse software module was used for image analysis. This allows us to take a series of overlapping images and merge them together into a seamless picture of the entire subject, so in this way tiled images can be enlarged in sections without resolution loss. To measure co-localization of components in the thrombi Manders' Colocalization Coefficient (MCC) was used as implemented by CoLocalizer Pro v7.0 (CoLocalization Research Software, Tokyo, Japan) and these coefficient values were quantified and statistically tested. Co-localization of two channels (red-green (NET-APC), red-blue (NET-CD66b), green-blue (APC-CD66b)) was evaluated with an algorithm, which calculates the signal intensity of pixels. Aspirated thrombi retrieved from 24 male patients were classified as fresh, lytic or organized and we collected data from at least three independent experiments per thrombus and from different thrombus areas to obtain images from central and peripheral thrombus regions, cell-rich and cell-poor regions as well. In fresh coronary thrombi, where pain-to-ballon time was less than 8 hours a strong signal corresponding to APC was observed and also clusters of monocytes (CD66b) were registered. Elements of NET were appeared only in a low amount in these thrombi (Figure 10).

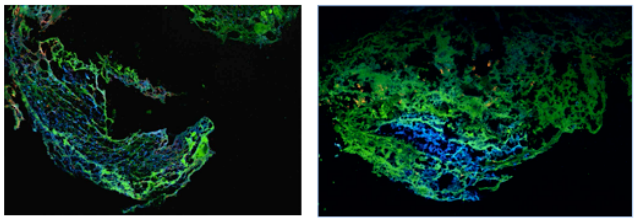

Figure 10. Immunofluorescent staining of fresh coronary thrombi.
APC appears in green, CD66b in blue and elements of NET (citrullined histones) in red.

In thrombi older than 8 hours presence of NET became more intense and cellular-rich regions were also larger (Figure 11). Here co-localization of APC and NET was moderate

with an average MCC2 of 0.526 (range 0.515-0.659), where MCC values correspond to the percentage of APC co-localized with the element of NET.

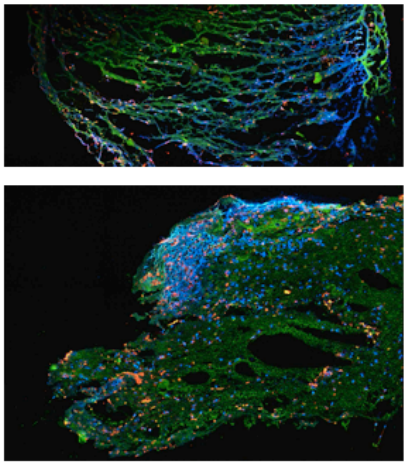

Figure 11. Immunofluorescent staining of thrombi older than 8 hours.
APC appears in green, CD66b in blue and elements of NET (citrullined histones) in red.

If thrombi were even older than 24 hours their structure was more heterogeneous, however the area covered by elements of NET was larger, and the amount of co-localized APC with NET was slightly, but statistically not significantly higher (MCC2 0.622, range 0.330-0.786).

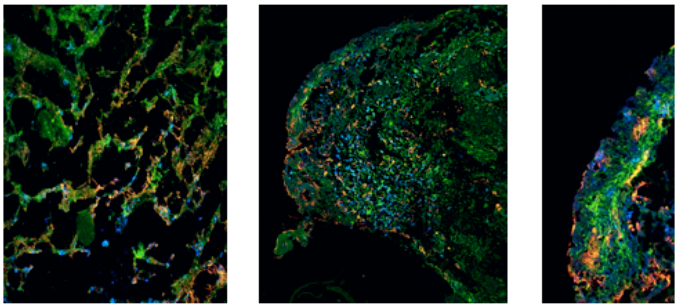

Figure 12. Immunofluorescent staining of thrombi older than 24 hours.
APC appears in green, CD66b in blue and elements of NET (citrullined histones) in red.

In summary, we could conclude from these data that APC is remarkably present in coronary thrombi, however the co-localization with NET is only moderate.